ISOTOPE EFFECTS ON CONFINEMENT AND TURBULENCE IN ECRH PLASMA OF LHD

K. TANAKA
National Institute for Fusion Science, National Institutes on Natural Sciences
Toki, Japan
Email: ktanaka@nifs.ac.jp

M. NAKATA, T. TSUJIMURA, H. TAKAHASHI, M. YOKOYAMA, R, SEKI, H. IGAMI, Y. YOSHIMURA, T. TOKUZAWA, T. AKIYAMA, I. YAMADA, R. YASUHARA, H. FUNABA, M. YOSHINUMA, K. IDA, M. GOTO, G. MOTOJIMA, M. SHOJI, S. MASUZAKI, M. OSAKABE, T. MORISAKI
National Institute for Fusion Science, National Institutes on Natural Sciences
Toki, Japan

Y.OHTANI
National Institutes for Quantum and Radiological Science and Technology
Naka, Japan

F. WARMER
Max-Planck-Institut für Plasmaphysik
Greifswald, Germany

Abstract

The positive isotope effects have been found in ECRH plasma of LHD. The enhancement factor of global energy confinement time (τ_E) to ISS04 scaling in deuterium (D) plasma is about 17% better than in hydrogen (H) plasma. Clear reduction of ion energy transport was observed, while electron energy transport does not change dramatically. The global particle confinement is degraded in D plasma. More hollowed density profiles were observed. It was not due to the neutral or impurity source, but due to the difference of the transport. Ion scale density fluctuation were measured and compared with gyrokineitc linear calculation. Spatial structure and collisionality dependence was similar both in H and D plasma. Fluctuation level was higher in D plasma. Quicker reduction with increase of collisionality and e-dia. propagating in plasma frame is qualitatively agree with TEM characteristics.

1. INTRODUCTION

The transport of different hydrogen isotopes is an important issue for predicting the performance of ITER and the future reactor operation. In a tokamak, improved transport character and lower H mode threshold power in D plasma than in H plasma were reported. Both tokamak scaling (ITER98y2) and helical scaling (ISS04) follow gyro-Bohm (GB) scaling with the exception of ion mass and ion charge number. While GB scaling predicts enhanced transport in D plasma, many experiments show better confinement (in tokamak) in D or comparable confinement (in medium-sized helical devices). In LHD, deuterium experimental campaign hast started from March 2017. Initial report about ECRH plasma with was reported in ref. 1 and 2. These results describe improvement in high power heating ECRH [1], scaling study and comparison with neoclassical transport [2] with some assistance of NB heating. This paper treats pure ECRH plasma, which are free from beam heating effects and describe the survey of particle transport and fluctuation characteristics in addition to energy transport.

2. ENERGY TRANSPORT

Figure 1 shows summary of global energy (τ_E). τ_E was estimated from diamagnetic stored energy and power deposition calculated by LHDGAUSS[3]. In the dataset, the contamination of helium is less than 5% and the purity of the H and D are higher than 80%, respectively. In the dataset, the injection power was 0.6-3.9MW in D, 0.8-3.8MW in H, $n_{e\,bar}$ was 0.6-3.7x10^{19}m^{-3} in D, 0.3-3.8x10^{19}m^{-3} in H. The one path absorption power was 92+-4% of injection power both for H and D plasma. Only one path absorption power was used for the τ_E estimation. The magnetic axis (R_{ax}) was 3.6m and Bt was 2.75T. The collisionality was normalized by the boundary between helical 1/ν and plateau regime at ρ = 0.5.

As shown in Fig.1 (a), τ_E is systematically higher in D. This is more apparent in the high collisionality regime. The improvement in D appears at ν_h^* ~>1, where neoclassical contribution becomes smaller and anomalous contribution becomes higher. As shown in Fig.1 (b), the hydrogen data sets almost follow ISS04 [4] scaling, while deuterium dataset is systematically higher than ISS04 prediction. The averaged enhancement factors are τ_E / $\tau_{E\ ISS04}$=1.27+-0.12 in D and 1.09+-0.02 in H plasma. Thus, improvement of τ_E in D to H is 17%. However, as shown in Fig. 1 (c), the enhancement factor depends on ν_h^*. The enhancement factor has a maximum at ν_h^* ~ 1.5 both in H and D plasma. Finally, the scaling was deduced from the dataset of 2017 campaign.

$$\tau_{E\ dia.ECH} \propto A^{0.24\pm0.01} \bar{n}_e{}^{0.58\pm0.01} P_{abs}^{-0.52\pm0.01} \quad (1)$$

Here, A is mass number (1 for H plasma, 2 for D plasma), $\bar{n}_e$ is the line averaged density, and P_{abs} is the absorption power.

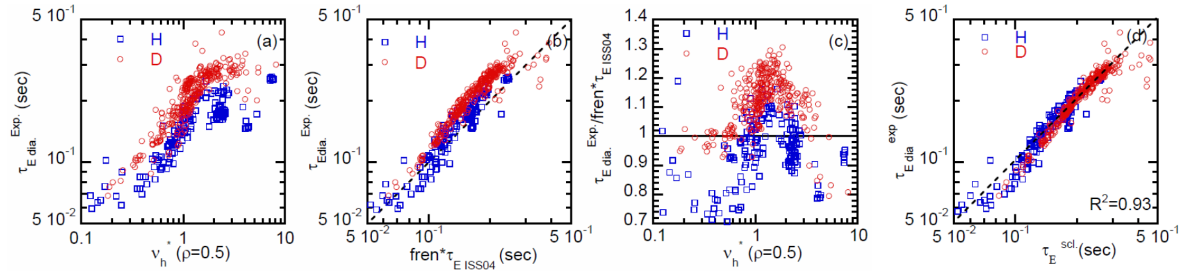

FIG. 1. τ_E of (a) collisionality dependence, (b) comparison with ISS04 scaling, (c) collisionality dependence of enhancement factor and (d) deduced scaling from the 2017 19th experimental campaign. In Fig.1 (b), fren is normalization factor of ISS04and is 0.93 for R_{ax}=3.6m [3].

Local power balance analysis was carried out by using TASK3D code [5] for the data set of density scan with 2.5MW (1MW 77GHz and 1.5MW 154GHz) heating. Density was scanned shot by shot. About 2sec flat top was obtained. Perpendicular NB was injected for 20msec for every 400ms for Ti measurements using CXRS. This short pulse injection is not to change Ti profile. Analysis timing was selected just before NB injection. Presently, n_e data of YAG laser Thomson scattering [6] is used for TASK3D. Figure 2 and 3 shows profiles of n_e, T_e, T_i and χ_e,χ_i. As shown in Fig.2 (a) and Fig.3 (a), n_e profiles are hollowed. This is widely seen in LHD [7]. Although, data points of Thomson n_e profiles are scattered, density profile is hollower in D plasma.

In low density case, as shown in Fig.2 (b), T_e and T_i profiles are almost identical. Ion heating is only due to the heat transfer from electron to ion. This heat transfer, which is equitation heating is show by the following equation [8].

$$P_{ei} \propto \frac{Z_i^2 n^2}{m_i T_2^{3/2}} (T_e - T_i) \quad (2)$$

Here, Zi is ion charge number, m_i is ion mass. Thus, for same density and same temperature difference between electron and ion, P_{ei} in H plasma is twice of those in D plasma. Similar density and almost identical T_i, as shown in Fig. 2(a) and (b) result in lower χ_i in D plasma as shown in Fig. 2(c). While χ_e is almost identical in H and D plasma as shown in Fig.2 (c).

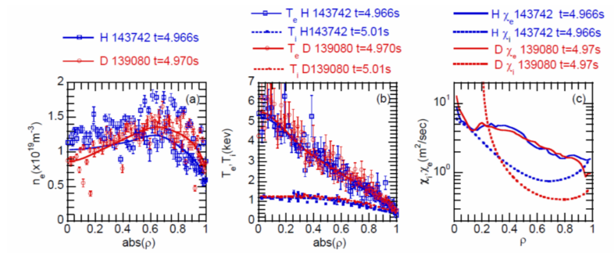

FIG.2 Low density case of (a) n_e,(b)T_e, T_i and (c) χ_e and χ_i profiles

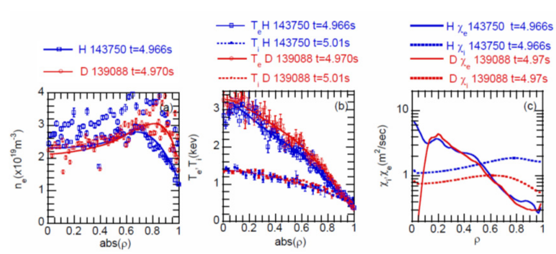

FIG.3 High density case of (a) n_e,(b)T_e, T_i and (c) χ_e and χ_i profiles

In high density case, T_e is higher in D plasma, T_i is almost identical, n_e profiles are hollower and edge n_e is higher in D region. These results in higher kinetic stored energy and better energy confinement in D plasma. As well as in low density case, χ_i is lower in D plasma. In low density case, χ_i is lower than χ_e in almost entire region, on the other hands, in high density case, χ_i is higher than χ_e at $\rho > 0.5$. These are common observation both in H and D plasma.

Figure 4 shows collisionality dependence of χ_e and χ_i at three radial locations. χ_e decreases with increase of ν_h^*. Both χ_e in H and D plasma shows same trend. While, χ_i in D plasma is lower at all location and all ν_h^* regime of present experimental data. At ρ = 0.5 and 0.7, χ_i increases with increase of ν_h^*. This is opposite tendency compared with χ_e. This tendency becomes moderate at ρ = 0.9. The difference of χ_e and χ_i become larger at more outer locations.

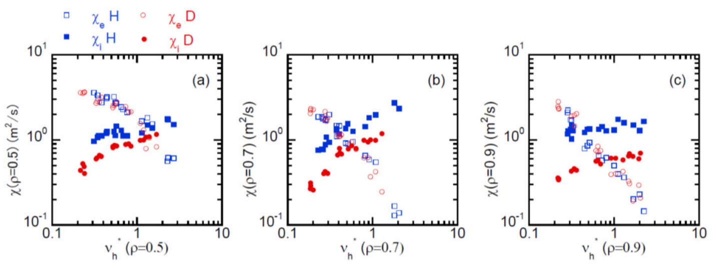

FIG.4 Collisionality dependence of χ_e and χ_i at (a) ρ = 0.5, (b) ρ = 0.7 and (c) ρ = 0.9

3. PARTICLE AND IMPURITY TRANSPROT

The global particle confinement time (τ_p) is estimated by the ratio between averaged density and amount of particle source in steady state. Two different estimation was used for particle source. One is by using neutral pressure gauge. Neutral pressure is an indication of edge particle source. Neutral pressure gauge is located in main vacuum vessel. The other is by using spectroscopic measurements. In the analysis method using spectroscopic data, particle source was estimated by the sum of the intensity of Hα, Dα and HeI lines. Then, τ_p was estimated for the data set of Fig.1 by using following equations.

$$\tau_p = \frac{N_e}{S_e - {dN_e}/{dt}} \simeq \frac{n_{e\,bar}}{Neutral\ Gas\ pressure}, \frac{n_{e\,bar}}{I_{H\alpha,D\alpha} + 2HeI} \tag{3}$$

Figure 5 (a) and (b) shows collisionality dependence of τ_p by using two different method. As shown in Fig.5 (a), τ_p from pressure gauge is clearly higher in H plasma. This indicates that neutral pressure is higher for same line averaged density in D plasma. This is partly due to the higher recycling rate and partly due to the lower pumping speed in D plasma. The pumping speed of the cryo-sorption pump is inversely proportional to square root of the molecular mass [9].

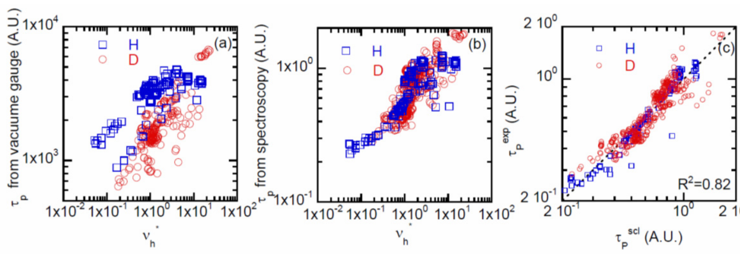

FIG. 5 τ_p of collisionality dependence (a) estimated from neutral pressure gauge, (b) estimated from spectroscopy, and (c) deduced scaling from spectroscopic τ_p.

While τ_p from spectroscopy does not show clear difference as shown in Fig.5 (b). However, the following scaling was obtained from regression analysis for the spectroscopic τ_p.

$$\tau_{P\ spec} \propto A^{-0.33\pm0.02} \bar{n}_e^{\ 0.52\pm0.02} P_{abs}^{-0.69\pm0.02} \tag{4}$$

It is big contrast that $\tau_{E\ dia}$ is 17% better in D plasma, τ_p spec is 20% worse for same $\bar{n}_e$ and P_{abs}.

Figure 6 (a)~(d) shows comparison of n_e and T_e profiels in H and D plasma. Low and high density cases are shown. In Fig.6(a) and (c), n_e profiles are from Abel inversion of multi-channel far infrared laser interferometer [10]. As shown in Fig. 6 (a)~(d), T_e profiles are almost identical in H and Plasma, however, n_e profiles are clearly different. Both in low and high density case, n_e profiles in D plasma is hollower. Also edge peak position of hollowed profiles, which is shown by the arrow, is more outwardly in D plasma. The particle source rate profile calculated by 3D Monte Carlo simulation code EIRINE shows that peak of the particle source is at ρ =1.05 where

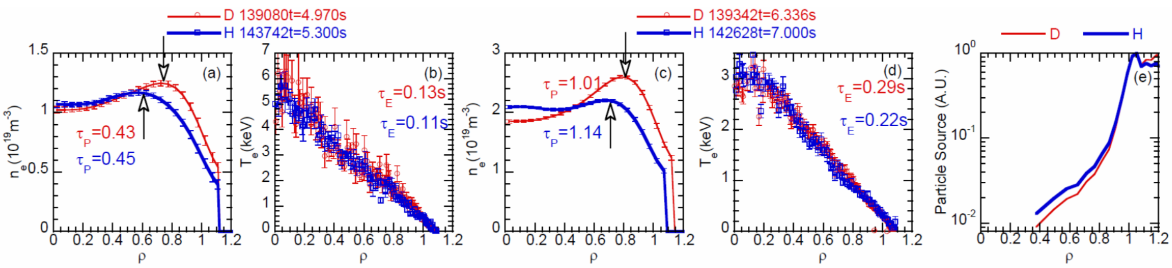

FIG.6 n_e and T_e profiles in (a),(b) low density, in (c),(d) high density and Particle source of D and H plasma is more outwardly of edge peak and the difference of neutral penetration is small as shown in Fig.5 (e). Thus, the difference of profile is not due to the difference of the neutral penetration of hydrogen or deuterium.

The effect of the impurity was investigated. The main impurity in core plasma of LHD is C_6^+. Main carbon source is carbon diverter plate. In D plasma, chemical and physical sputtering at divertor plate is enhanced. Then, In-flux of carbon is higher in D plasma than in H plasma [11]. Figure 7 (a) shows electron density from C_6^+ions ($6n_c$, where n_c is C6+ density from charge exchange spectroscopy). $6n_c$ is higher in D plasma due to the larger carbon influx. As well as n_e profiles, $6n_c$ is hollower in D plasma. However, difference of $6n_c$ does not account for the difference of n_e profile. Because as shown in Fig.7 (b), in D plasma 139088, edge peak density is $0.22x10^{19}m^{-3}$ lower than edge peak density of H plasma, however, edge 6nc is $0.062x10^{19}mm^{-3}$ higher. Thus, figure 6 and 7 indicate that hollower n_e profiles in D plasma is not due to the difference of particle source but due to the difference of transport.

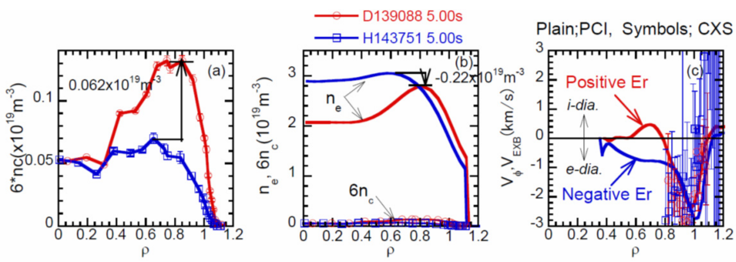

FIG.7 Comparison of (a) electron density profile ionized from $C_6^+(6n_c)$, (b) n_e and $6n_c$ and (c) turbulence phase velocity, E_rxB_t poloidal rotation velocity.

Figure 6 (c) shows turbulence phase velocity measured by two dimensional phase contrast imaging (2D-PCI) [12,13]. E_rxB_t poloidal rotation speed profiles measured by charge exchange spectroscopy [14] are over plotted. 2D-PCI measures ploidal dominated wavenumber, thus measured phase velocity indicates fluctuation phase velocity Doppler shifted by E_rxB_t rotation. Thus, the measured phase velocity can be indicator of E_r. As shown in Fig.6 (c), in D plasma, where $6n_c$; is extremely hollowed, phase velocity is ion diamagnetic propagation in labolatory frame which suggests positive E_r, if turbulence phase velocity is dominated by E_rxB_t rotation. While in H plasma, where $6n_c$ is not hollowed but flat, the phase velocity is electron diamagnetic propagation, which suggests negative E_r. One possible interpretation of hollower $6n_c$ is due to the neoclassical effects of positive E_r, which transfer positively charged impurity ion outwardly.

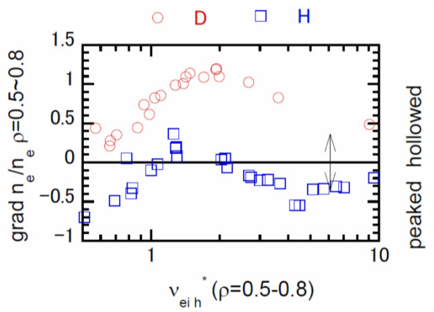

FIG.8 Collisionality dependence of normalized density gradient

Figure 8 shows the ν_h^*dependence of normalized gradient (grad n_e/n_e) at ρ = 0.5-0.8, where grad n_e/n_e varies significantly. In whole experimental regime grad n_e/n_e is higher in D plasma. Both in H and D plasma grad n_e/n_e once increases then decreases. This is a clear contrast grad n_e/n_e decreases (density peaking factor decreases) monotonically with increase of ν_h^* in NBI plasma [15].

Finally, density modulation experiments were performed in order to estimated diffusion coefficients and convection velocities. Modulation frequency was set to be 2.5Hz. The data set of a pair of comparison are shown in Fig.9 (a) ~ (c). The equilibrium profiles are hollower in D plasma as shown in Fig.9 (a). But the difference of modulation amplitude and phase is much clearer as shown in Fig.9 (b) and (c). This indicates that the density modulation is more sensitive to the difference of the particle transport than equilibrium profiles. However, flattening or reversal of the modulation phase, which is seen at ρ < 0.5 as shown in Fig.9 (c), make the determination of diffusion coefficients (D_{mod}) and convection velocity (V_{mod}) difficult. Presently, estimation are limited in edge region. The following scaling was obtained for D mod at ρ = 0.8-1.0.

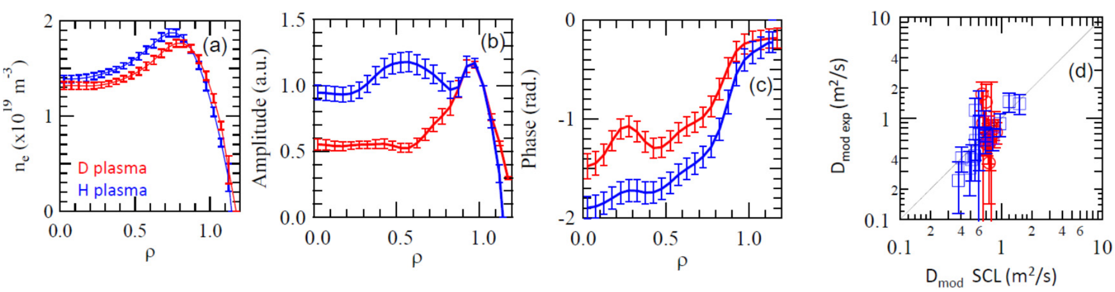

FIG.9 Density modulation experiments: Comparison of (a) equilibrium profile, (b)modulation amplitude, (c) modulation phase and (d) deduced scaling of modulation diffusion coefficient at ρ = 0.8 - 1.0.

$$D_{mod\ at\ \rho\sim 0.8-1.0} \propto A^{0.68}\bar{n}_e^{-1.02}T_e^{-0.52} \quad (5)$$

D_{mod} is higher in D plasma for same n_e and T_e. This is qualitatively consistent with scaling of global particle confinement time shown by eq. (4).

3. TURBULENCE

Ion scale turbulence such as ITG or TEM can play a role on energy, particle and impurity transport. The 2D-PCI measures the turbulence of k = 0.1 – 0.8 mm^{-1} corresponding to $k\rho_i \sim 0.08\sim1.04$ for H and 0.12~1.6 for D plasma, f = 20 – 500 kHz at ρ >~ 0.4. The CO_2 laser beam passes the vertically elongated cross section and measures turbulence from both the upper and the lower side relative to the equatorial plane.

Fig.10 shows n_e, T_e, T_i and fluctuation profiles in low and high density D plasma. In Fig. 10 (a-5) and (b-5), $E_r xB_t$ poloidal rotation velocity (V_{EXB}), which is measured by HIBP [16] and CXRS[14], are over plotted. V_{EXB} in Fig (a-5) and (b-5) are projected components to the measured wavenumber of 2D-PCI. In low density case, as shown in Fig. 10 (a-5), dominant components exists at ρ ~ 0.5 and propagates toward the ion diamagnetic direction (i-dia.) in laboratory frame. At same location, V_{EXB} from HIBP shows further i-dia. propagation. This suggests that fluctuatin at this location propagates toward the electron diamagnetic (e-dia.) direction in plasma frame. This is one of the characteristics of TEM.

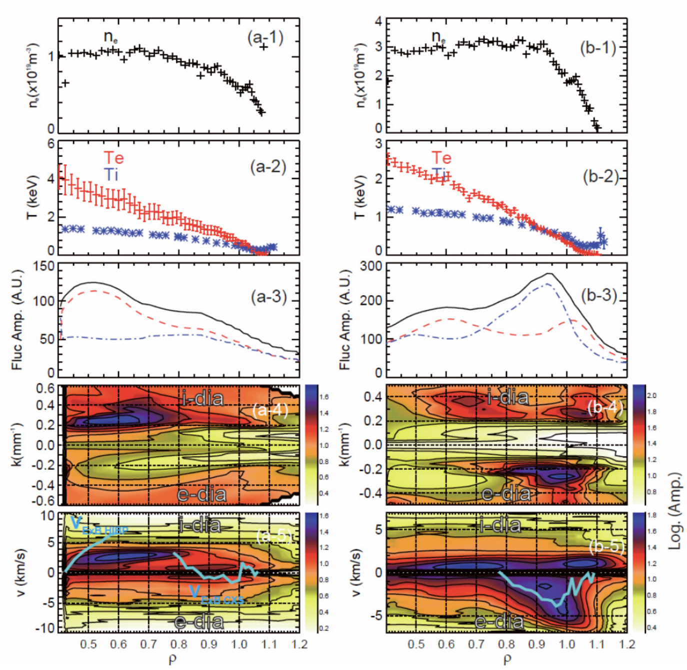

FIG. 10 Profiles in low density (a-1)~(a-5) and high density H (b-1)~(b-5) of hydrogen ECRH plasmas. (a-1),(b-1) n_e, (a-2),(b-2) T_e and T_i profiles, (a-3),(c-3) electron density fluctuation amplitude, (a-4), (d-4) contour plot of fluctuation amplitude k spectrum and (a-5), (b-5) contour plot of fluctuation amplitude phase velocity in laboratory frame. In (a-3), (b-3), plain black dashed red and dotted blue lines indicate, total, e-dia, and i-dia. components respectively. In (a-5), (b-5), blue lines indicate $E_r xB_t$ poloidal rotation velocities measured by HIBP and CXRS.

In high density case, fluctuation profiles changes significantly. Core i-dia. components at ρ = 0.4 - 0.7 decreases, edge e-dia. at ρ =0.8 - 1.1 components increases and edge i-dia. peak (ρ ~ 1.05) appears. Fluctuation phase velocity almost follows V_{EXB} from CXRS as shown in Fig. 10 (b-5). These spatial structure is similar both in H and D plasma. Presently, the measured peak wavenumber is almost identical, while ion Larmor is factor 1.4 higher in D plasma.

Figure 11 shows comparison of fluctuation behaviour in density ramp up plasma of H and D plasma. Density was ramped up from 1 to $4x10^{19}m^{-3}$ in D and from 1 to $3.5x10^{19}m^{-3}$ in H plasma. Change of the fluctuation spatial profiles with change of the density are clearly visible. In low density phase, core i-dia. fluctuation, of which peak position is ρ ~ 0.7 dominates. The core i-dia. components decreases with increase of the density. While edge e-dia.

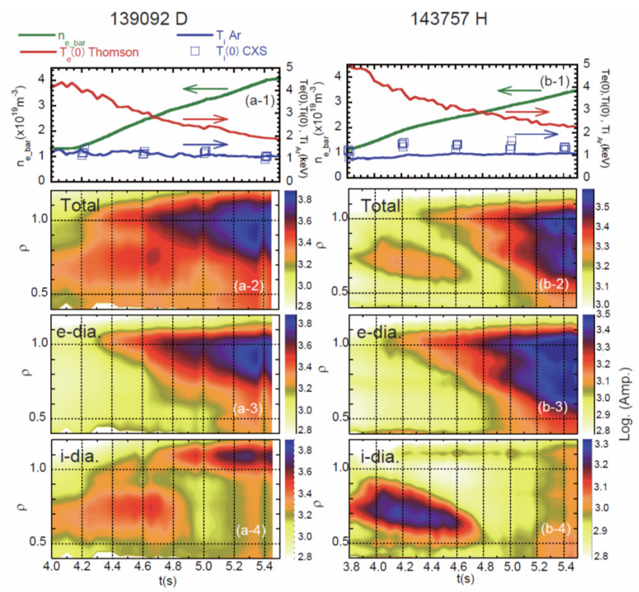

FIG.11 Time history of (1) n_e, T_e,T_i, (2) total , (3) e-dia. and (4) i-dia. fluctuation amplitude. (a-1)~(a-4) in D and (b-1)~(b-4) in H plasma

components, of which peak is at ρ ~ 1.0 at initial stage, increases with increase of the density. The edge e-dia. components spreads toward the core region with increase of the density.

Figure 12 shows collisionality dependence of fluctuation level, which are fluctuation amplitude normalized by background density, in H and D plasma. The fluctuation components are total including both e-dia. and i-dia. components. The data of Fig.12 consists of density scan shot by shot in Fig. 4 and density ramp up data in Fig.11. All data are 2.5MW (1MW 77GHz, 1.5MW 154GHz) ECRH injection. As shown in Fig. 12 (a), core (ρ = 0.5-0.8) fluctuation level decrease with increase of ν_h^* up to ν_h^*~2, then, core fluctuation level increases with increase of ν_h^*. The former decreasing phase is decrease of core i-dia. components and latter increasing phase is increase and spreading edge e-dia. components as shown in Fig.11.

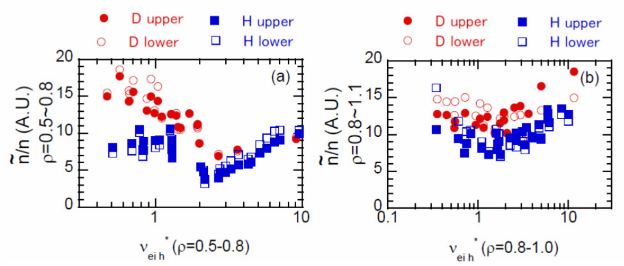

FIG. 12 Collisionality dependence of fluctuation level at (a) ρ = 0.5-0.8 and (b) 0.8-1.1

Present data set shows fluctuation level in D plasma is higher almost entire ν_h^* region. Core fluctuation level in D plasma decreases more rapidly up to ν_h^*~2, than in H plasma. Gyro kinetic analysis showed stronger collisionality stabilization of TEM in D plasma [17] and qualitatively consistent with observations.

Edge fluctuation also once decrease up to ν_h^*~2, then increases with increase of ν_h^*. As well as core turbulence, former decreasing phase is due to the increase of i-dia. core components, latter increase is due to the increase of edge e-dia. components.

Gyrokinetic linear calculations were carried out by using GKV code. GKV is local flux tube gyrokinetic code. In present calculation, kinetic electron, collisionality effects are included. Ion species are only H and D. Detail results and calculation process are reported in ref. 18. Linear growth rate were calculated for low and high density in H and D plasma. These are same shot of Fig.2 and 3. But, density profiles by FIR laser interferometer was used. Gyrokinetic calculation is very sensitive to the density and temperature gradient, thus, all profiles (n_e, T_e and T_i) are accumulated for 1 sec in order to use accurate profile. Fluctuation level was also accumulated for 1sec.

The results of low and high density cases are shown in Fig. 13 Fig.14 respectively. Calculated was performed for $k\rho_i$=0.1~1.5. The measured regions of $k\rho_i$ are $k\rho_i$ ~ 0.08~1.04 for H and 0.12~1.6 for D plasma. Almost both calculation and measurements region correspond each other. In Fig.13 (d) - (g) and Fig.14 (d)-(g), growth rate is same unit both for H and D plasma. The hydrogen thermal velocity was used for the normalization. Hydrogen and deuterium mass was used for ρ_i in H and D plasma respectively. The calculation was carried out at four different at ρ = 0.36, 0.5, 0.7 and 0.9.

As shown in Fig.13 (d) ~ (f), core fluctuation components in low density case at ρ = 0.36-0.7 are TEM and ITG, while experimentally the core components propagates e-dia. direction in plasma frame suggesting TEM characteristics. The growth rate is higher at ρ = 0.36 and 0.7 in H plasma and comparable at ρ = 0.5, while

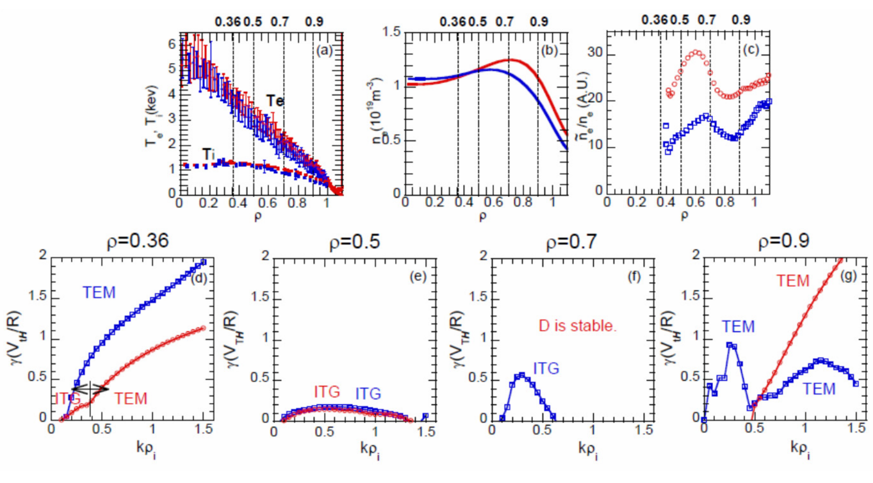

FIG. 13 Profile in low density case of (a) T_e, T_i,(b)n_e,(c) fluctuation level and (d)~(g) linear growth rate at ρ=0.36, 0.5,0.7 and 0.9 H 139080 (t=4.4-5.4s), D 143742(t=4.5-5.5s). Red is D, Blue is H.

fluctuation level is higher in D plasma. The growth rate is the highest at ρ = 0.36, while the peak of the measured core fluctuation level is at ρ =0.6.

Figure 13 (g) shows growth rate at ρ = 0.9, where e-dia. propagating edge components exist. TEM is dominant instability at this location. In D plasma, the region at $k\rho_i < 0.5$ is stable. At $k\rho_i > 0.5$, growth rate is higher in D plasma. Measured fluctuation level is higher at this location as well.

Figure 14 (d), ρ = 0.36 of high density case is hybrid of ITG and TEM. At this location, growth rate is clearly higher in D plasma. At ρ = 0.5, growth rate becomes comparable in H and D plasma as shown in Fig.14 (e), and location ρ = 0.7 becomes stable. At ρ = 0.9, dominant instability is TEM and growth rate is comparable in H and D plasma. While measured fluctuation level is higher in D plasma in all radial locations.

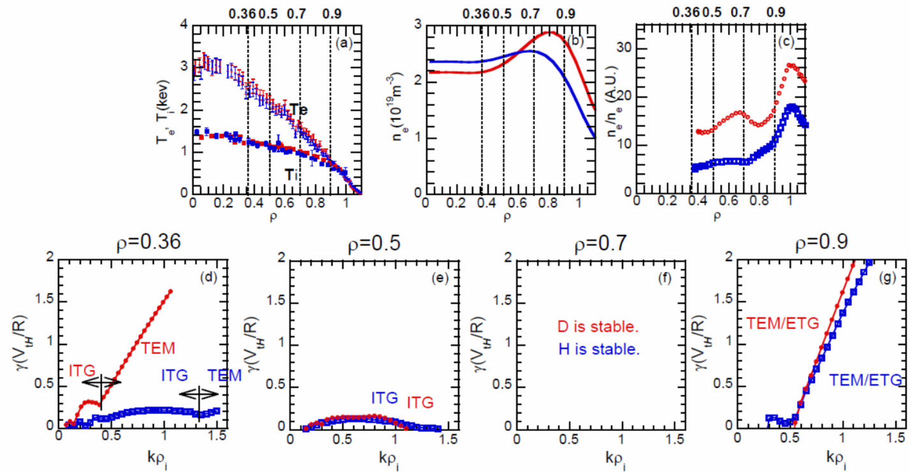

FIG. 14 Profile in low density case of (a) T_e, T_i,(b)n_e,(c) fluctuation level and (d)~(g) linear growth rate at ρ=0.36, 0.5,0.7 and 0.9 H 139080 (t=4.4-5.4s), D 143742(t=4.5-5.5s . Red is D, Blue is H

4. DISCUSSION AND SUMMARY

Extensive investigation of isotope effects were performed for ECRH plasma of LHD. Unlike tokamak, ELM and MHD activity such as sawteething do not appear and do not disturb plasma, thus, precise comparisons are possible. The data at analysis timing was free from beam heating effects. Thus, present data set is purely external electron heating plasma. Global energy confinement time is 17% higher in D plasma than in H plasma. Power balance analysis for density scan dataset with constant injection power showed comparable χ_e and reduced χ_i in D plasma. Ref.1 and Ref.2 reports that injection direction of tangential ECRH play a role on the isotope effects. This suggests that iota profile affects isotope effects. Recent analysis about NB heating plasma showed that τ_E does not show ion mass dependence [19]. This is clear contrast to the result of ECRH plasma described in this paper. This may suggests isotope effects varies on heating channel. Further investigation is necessary for the comprehensive understanding of isotope effects of LHD

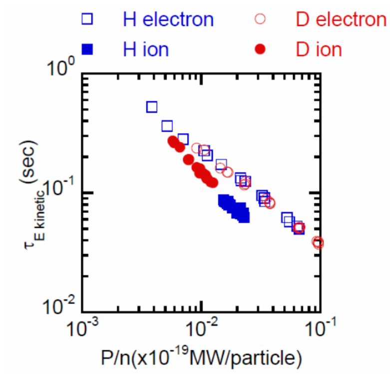

FIG. 15 Power degradation of kinetic ion and electron energy confinement time

In ASDEX-U ECRH heating plasma, better confinement was observed in D than in H plasma. However, the observed difference is due to the difference of the equipartition heating. Higher equipartition heating in H plasma results in larger power degradation and enhanced transport [20]. In order to investigation of power degradation of ion and electron energy transport in LHD, kinetic confinement times was compared for the density scan data set. The results are shown in Fig. 15. The dataset of Fig. 15 is is same datasets of Fig. 4. Kinetic electron energy confinement time of H and D plasma overlaps in the same trends. While ion kinetic electron energy confinement time power does not overwrap. However, H and D data set lines also same trend. This observation suggests similar underlined mechanism exists to ASDEX-U results. Power degradation is stronger in ion channel.

Particle transport is enhanced in D plasma. This is confirmed by three different analysis technique (τ_p from neutral pressure gauge, τ_p from spectroscopy and edge diffusion coefficients from density modulation). This is clear contrast to the reduced global energy transport in D plasma. Density profiles are hollower in D plasma. But this is not due to the impurity but due to the difference of particle transport of bulk ions.

Ion scale turbulence was measured by using 2D-PCI. Two different components in core and edge region were found. Fluctuation spatial structure change with increase of density or collisionality. In low density, i-dia, propagating components dominates in core region at $\rho = 0.5$-0.8. This propagates e-dia. direction in plasma frame. Core i-dia. components decrease with increase of collisionality. With increase of the density, edge e-dia. propagating components at $\rho = 0.8$-1.1 becomes lager and spreading from edge to core region. These characteristics are in H and D plasma. Different fluctuation characteristics in core and edge region are also seen in NB heated plasma [21]. Present data set shows higher fluctuation level in D plasma.

Gyrokinetic linear analysis was performed. Experimentally, core i-dia. components shows characteristics of TEM. But correspondence to linear calculation is not clear. More detail parameter surveys are necessary both for experimental data and linear calculations.

ACKNOWLEDGEMENTS

This work is supported by NIFS grants NIFSULHH013, NIFS10ULRR702, NIFSULHH004, ULHH005, ULHH02 ULHH028, NIFS16KLER045 and NIFS14UNTT006 and JSPS grant 16H04620

REFERENCES

[1] TAKAHASHI, H., et al, Nucl. Fusion **58** (2018) 106028
[2] WARMER, F., et al, Nucl. Fusion **58** (2018)106025
[3] TSUJIMURA, T., et al, Nucl. Fusion 55 (2015) 123019
[4] YAMADA, H. et al, Nucl. Fusion, **45**, (2005)1684.
[5] YOKOYAMA, M. et al, "Extended Capability of the Integrated Transport Analysis Suite, TASK3D-a, for LHD Experiment, and its Impacts on Facilitating Stellarator-Heliotron Research"[FIP/P7-35], paper presented at 25th IAEA Int. Conf. on Fusion Energy, Saint Petersburg, 2014
[6] YAMADA, I. et al, Fusion Sci. Tech. **58**, (2010) 345
[7] TANAKA, K. et al, Fusion Sci. Tech. **58**, (2010), 70
[8] WESSON J.A. 1997 Tokamaks 2nd edition (Oxford: Clarendon)
[9] MOTOJIMA, G. et al, this proceeding
[10] TANAKA, K. et al, Plasma Fusion Res **3**, (2008) 050
[11] MASUZAKI, S. presented at 21st Int. Stellarator–Heliotron Workshop (Kyoto, Japan 2–6 October 2017)
[12] TANAKA, K. et al, Rev. Sci. Instrum. **79**, (2008), 10E702
[13] MICHAEL, C. et al, Rev. Sci. Instrum. **86**, (2015), 093503
[14] YOSHINUMA, M. et al, Fusion Sci. Tech. **58**, (2010) 37
[15] TANAKA, K. et al, Fusion Sci. Tech. **58**, (2010), 70
[16] IDO, T. et al, Fusion Sci. Tech. **58**, (2010), 436
[17] NAKATA, M et al, Phys. Rev. Lett. **118**, (2017), 165002
[18] NAKATA, M et al, Plasma Phys. Ctrl. Fusion in press
[19] YAMADA, H. et al, this proceeding.
[20] SCHNEIDER, P.A. et al, Nucl. Fusion **57** (2017) 066003
[21] TANAKA, K. et al, Nucl. Fusion **57** (2017) 116005